Structure and dynamics of the hyaluronan oligosaccharides and their solvation shell in water: organic mixed solvents

Structure and dynamics of the hyaluronan oligosaccharides and their solvation shell in water:organic mixed solvents

Eva Kutálková[a], Marek Ingr[a,b,*], Alena Kolaříková[a], Josef Hrnčiřík[a], Roman Witasek[a], Martina Hermannová[c], Ondřej Štrympl[c,d], Gloria Huerta-Ángeles[c,e]

[a]Tomas Bata University in Zlín, Faculty of Technology, Department of Physics and Materials Engineering, Nám. T.G. Masaryka 5555, 76001 Zlín, Czech Republic

[b]Charles University, Faculty of Science, Department of Biochemistry, Hlavova 8/2030, 12840 Praha 2, Czech Republic

[c]Contipro a.s., Dolní Dobrouč 401, 561 02 Dolní Dobrouč, Czech Republic

[d]Charles University, Faculty of Science, Department of Physical and Macromolecular Chemistry, Hlavova 8/2030, 12840 Praha 2, Czech Republic

[e]Institute of Macromolecular Chemistry, CAS AS CR, Heyrovského nám. 2, 162 06, Praha 6, Czech Republic.

Abstract

Hyaluronan (HA) is a natural polysaccharide occurring ubiquitously in the connective tissues of vertebrates widely used in the cosmetic and pharmaceutic industries. In numerous applications HA oligosaccharides are being chemically modified using reactions incompatible with aqueous solutions, often carried out in water:organic mixed solvents. We carry out molecular-dynamics (MD) simulations of HA oligosaccharides in water:1,4-dioxane and water:tert-butanol mixtures of different compositions. HA molecule causes a separation of the solvent components in its surroundings, especially in tert-butanol containing solutions, constituting thus a solvation shell enriched by water. Furthermore, interactions with ions are stronger than in pure water and depend on the solvent composition. Consequently, the dynamics of the HA chain varies with the solvent composition and causes observable conformational changes of the HA oligosaccharide. Composition of mixed solvents thus enables us to modify the interaction of HA with other molecules as well as its reactivity.

Keywords: hyaluronan, mixed solvent, molecular dynamics, solvent separation, 1,4-dioxane, tert-butanol

1. Introduction

As a highly hydrophilic polysaccharide, hyaluronan (HA) is most often studied in aqueous solutions. In this environment HA forms highly swollen random coils and its macromolecular chain strongly prefers interactions with water to those with other parts of the same or other macromolecule. It was shown by numerous experimental works (Fouissac et al., 1992; Hayashi et al., 1995; Mendichi et al., 2003) providing the description of HA random coils, especially their radii of gyration R_g, corresponding with our previous molecular-dynamics (MD) study presuming a model of a non-interacting chain (Ingr et al., 2017). In accord with this, tertiary structures of HA oligo- or polysaccharides are thermodynamically unstable in aqueous solution and are nowadays considered not to exist at all (Blundell et al., 2006; Gribbon et al., 2000), although some authors declared their identification (Scott & Heatley, 1999, 2002). The semi-rigid nature of the HA chain, whose rigidity decreases along with the increasing salt concentration in the solvent (Buhler & Boué, 2004), is stabilized by intramolecular hydrogen bonds, but likely also by HA-water hydrogen bonds anchoring the molecule to a well-structured solvation shell (Kutálková et al., 2020). In that work we show that regions of organized water exist both around the hydrophilic and hydrophobic epitopes of HA molecule and thus wrap it into a shell protecting the HA molecule from intermolecular interactions. Even ions are in general repelled from the HA surface behind this first solvation shell except for several specific positions where the Na^+ cations are attracted electrostatically either by the charged carboxylate group or by the partial negative charges of other oxygen atoms. This makes HA not only highly soluble, but also rather inert to interactions with other molecules. Mutual interactions between HA chains are enabled, although still weak, only at higher ionic strength (Kolaříková et al., 2022). At low salt concentration HA interacts firmly only with highly specific binding sites of its protein receptors called hyaladherins. For technological applications HA is thus often modified chemically in order to change its

physicochemical properties (Payne et al., 2018; Svechkarev et al., 2018; Štrympl et al., 2021). The chemical syntheses are not always feasible in aqueous solutions but should be carried out in environments containing a fraction of various organic solvents (Kutálková et al., 2021; Schanté et al., 2011; Štrympl et al., 2021). Such mixed solvents, however, represent environments deprived of water and the behavior of HA in them may be different. Although the mixed solvents are often used even within other technologically relevant processes (Bicudo & Santana, 2012; Hu et al., 2009; Vítková et al., 2019), to our knowledge no MD simulation of HA in these environments has been carried out yet except for our previous study (Kutálková et al., 2021). Only few simulations of HA in solvents containing different molecules than water and salts were carried out, investigating the interaction of HA with phospholipids in the synovial fluid (Siódmiak et al., 2017; Bełdowski et al., 2019; Siódmiak & Bełdowski, 2019). Therefore, investigation of HA in mixed water:organic solvents opens a perspective research direction the results of which may contribute to understanding various solvent-composition dependent physicochemical phenomena including chemical reactivity (Kutálková et al., 2021; Štrympl et al., 2021) and can be exploited to design optimum conditions of different technological processes.

In this work we carry out the first systematic MD study of HA oligosaccharides in two mixed solvents, water:1,4-dioxane (dioxane, DX) and water: 2-methylpropan-2-ol (tert-butanol, TB) in order to describe their conformation, solvation shell and interactions with the solvent components. This study is a continuation of our previous work (Kutálková et al., 2021) aimed at providing an explanation of the results obtained thereof on the molecular basis. Our aim is to show that different mixed solvents undergo different component separation in the solvation shell of HA and change differently the properties of HA compared to aqueous solutions.

2. Methods

Molecular-dynamics (MD) simulations

All MD simulations were carried out by NAMD 2.10 program package (Phillips et al., 2005). CHARMM 36 force field was used for the HA molecule, CGenFF topology and parameter files were used for the 1,4-dioxane and tert-butanol molecules (used also in previously reported studies (Bakulin et al., 2021; Kutálková et al., 2021; Overduin et al., 2019)), TIP3P model of water was applied. First, equilibration of the boxes of pure mixed solvents were carried out. HA was then wrapped by these boxes to form the complete simulation box. The energy of each system was minimized for 5400 fs prior to the MD simulation. Integration was performed by the Verlet-I/r-RESPA MTS method with the slow-force mollification, a timestep of 1 fs for bonding and 2 fs for non-bonding interactions and 10 Å cutoff of non-bonding interactions was used. Full electrostatic calculations were performed every 6^{th} fs using the Particle Mesh Ewald (PME) method. The simulations were run for at least 200 ns at NpT ensemble, the initial dimensions of the simulation box were approx. $100 \times 100 \times 100$ Å^3. The pressure (1 atm in all the simulations) was controlled using the Langevin piston Nosé-Hoover method and the temperature was controlled using Langevin dynamics.

HA oligosaccharides of 20 monosaccharide units were simulated in altogether 7 different solvents, pure water and three compositions of water:dioxane and water:tert-butanol solutions, in both cases with volume fractions of the organic components of 0.33, 0.50, 0.67 (the volume to volume ratios 2:1, 1:1 and 1:2, respectively). This choice is in accord with our previous study (Kutálková et al., 2021) which revealed different HA reactivity in the individual mixtures. Experimentally, the esterification reaction of HA is usually performed in a mixture of solvents composed of an organic polar solvent mixed with water (Huerta-Angeles et al., 2014). Furthermore, it was observed that the esterification reaction of high molecular weight

HA is more efficient in low permittivity ether solvents such as tetrahydrofuran or dioxane rather than in alcohols and the regularity of the substituent distribution was influenced, too (Štrympl et al., 2021). Therefore we chose one representative of each group.

The simulations were carried out at two temperatures, 310 K (37 °C – physiological temperature) and 277 K (4 °C – chosen to be as low as possible but still above the melting point of all the mixtures). The choice of the two different temperatures was further supported by the coherence with experimental studies searching for the optimum conditions that must consider two effects that decrease the reaction rate – higher entanglement of HA chains at low temperature causing increased viscosity impairing the diffusion of reagents and the decrease of the stability of the reaction intermediates and thus the substitution yield at high temperature (Peydecastaing et al., 2011). Simulations of HA oligosaccharides in salt-free solvent contained 10 Na^+ cations compensating the negative charge of HA while simulations in 0.1 M NaCl contained 70 Na^+ cations and 60 Cl^- anions. (NaCl was chosen as the most common salts with well reliably verified force fields. Moreover, HA is found naturally as sodium hyaluronate, therefore the majority of experimental studies with HA are done in the environment of Na^+ ions.) For simulation details see Table S1. The simulation results were visualized and certain analyses were carried out using the VMD program (Humphrey et al., 1996), also used to determine the numbers of hydrogen bonds. The donor-H-acceptor group of atoms was considered as a hydrogen bond if the distance between the donor and acceptor was up to 3 Å and the deflection from the straight angle on the hydrogen atom up to 20°. Mean values of different characteristics (end-to-end distance, numbers of hydrogen bonds, ions within a given distance from HA) were evaluated from 3000 frames covering the last 100 ns of the simulation. Their standard deviations of the mean are thus smaller than the symbols in the graphs.

Solvation shell of individual residues of HA oligosaccharides was studied using the cumulative solvation-shell diagrams (CSSD) the construction of which was described previously (Kutálková et al., 2020). In brief, all the residues from all recorded simulation frames (in this case 600 frames covering 50 ns of the equilibrated part of the simulation) are viewed in the same orientation together with the solvent molecules, all these individual images are superimposed and projected to a plane perpendicular to the viewing direction. Atoms of different kinds are plotted in different colors in order to localize the positions of their frequent occurrence. For details see section SM1.

3. Results and discussion

3.1. Solvent components around the HA oligosaccharide

Distribution of solvent molecules around the HA chain was studied for three different compositions of both kinds of the mixed solvents at two different temperatures and two different NaCl concentrations. All the results are presented in Fig. 1 by means of radial distribution functions (RDFs) of water and organic components.

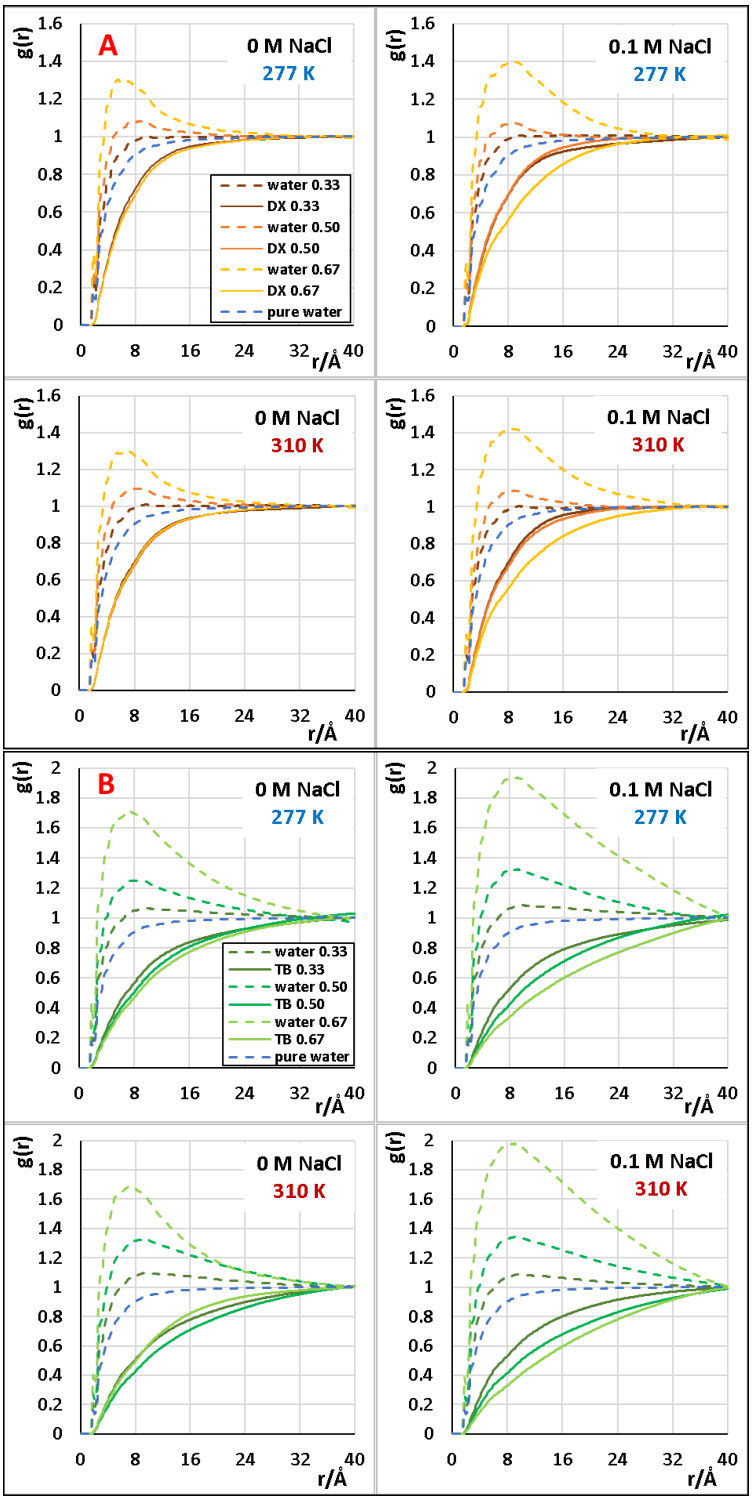

Fig. 1. Radial distribution functions of water and the organic components (A – dioxane, B – tert-butanol) in the solvation shell of the HA molecule in mixed solvents of different composition (indicated in the legends of the plots - the words (acronyms) indicate the components related to individual curves and the numbers the volume fraction of the organic component).

157

158 A clear common feature of all the systems is the increased concentration of water in the

159 surroundings of HA while the organic component is repelled from this area. As we showed

previously (Kutálková et al., 2021), this separation is remarkably stronger in water:tert-butanol mixture. The maximum of the water RDF is located at approx. 8 Å for all the systems but its value for tert-butanol solutions is always considerably higher than for the corresponding dioxane mixtures. In case of water:dioxane salt-free solution the dioxane RDFs are identical for all the solvent compositions and their temperature dependence is negligible, too (Fig. 1). It indicates that within the considered concentration range the dioxane molecules behave independently, each one as if it was alone in the solution. The molar excess of water in the HA proximity grows with the dioxane concentration as a consequence of the smaller size of the water molecule. This behavior shows that water defines the primary environment around HA which determines the distribution of dioxane molecules protecting them from their mutual interactions. It is likely caused by strong solvation of the dioxane molecules on its oxygen atoms which, together with the symmetrical shape of the molecules, hinders the hydrophobic interaction between them. When the solution contains 0.1M NaCl, the ions attracted by HA bind some water to their own solvation shells pushing thus the dioxane molecules farther from HA and increasing slightly the maximum of RDF of water. This phenomenon is apparent comparing the dioxane RDFs for the volume fractions of 0.67 on one hand and 0.33 and 0.50 on the other hand. Temperature dependence of the discussed phenomena is negligible indicating that the solvation-shell reorganization around HA is accompanied with only a small enthalpy change, i.e. a small difference in the energy of non-covalent interactions of the molecules participating in this process, and is thus driven rather entropically, i.e. by the tendency to reach a maximum possible disorder.

In water:tert-butanol solutions, both with and without 0.1 M NaCl, the tert-butanol radial distribution functions have generally lower values than their dioxane counterparts and are dependent on the mixture composition. For the tert-butanol volume fractions of 0.33 and 0.50 the trends of the RDFs are qualitatively similar, the one for 0.50 lies lower indicating

relatively higher repulsion of tert-butanol by HA when less water is present in the system. It indicates the mutual hydrophobic interactions of the amphiphilic tert-butanol molecules stabilizing the solution by the formation of temporary clusters whose stability is supported by tert-butanol concentration. This behavior resembles the phase separation of the mixtures of limited-miscibility liquids which, however, takes place only in the close vicinity of HA for tert-butanol. In the tert-butanol-richest solution (volume fraction 0.67) the described tendency is kept in all the studied systems except for the salt-free solution at 310 K where the RDF of tert-butanol gets higher than expected – the tert-butanol fraction in the solvation shell is even the highest from all the solutions. It is likely a consequence of the more intense thermal motion of the molecules leading to a more extensive mixing of the molecules that cannot be overwhelmed by the hydrophobic forces. In the salt-containing solutions the differences between the individual RDFs are larger, obviously due to the higher polarity of the solution and stronger hydrophobic interactions. Consequently, no anomalous order of the RDFs is observed in 0.1 M NaCl.

A spectacular comparison of the two kinds of mixed solvents is given in Fig. 2 where the absolute molar concentrations of the components are shown as functions of the distance r from the HA molecule. The concentration of water reaches its maximum at 5-10 Å for all the systems. In the dioxane-containing solutions the maximum concentration shows a notable difference from the free-solvent concentration only for the highest dioxane fraction. On the contrary, the maximum water concentration of the tert-butanol-containing solutions differs significantly from its free-solvent values but its differences among the different tert-butanol fractions are remarkably lower. It indicates again the strong solvent separation tending to wrap the HA molecule by as much water as possible. Furthermore, when 0.1 M NaCl is added, the mixed solvents separate more strongly around HA since the higher polarity of the solvent results in a stronger attraction between HA and water (including the dissolved cations)

and an increased repulsion of the organic molecules from HA due to the intensified hydrophobic forces. While in dioxane-containing solutions this change is rather low, in solutions of tert-butanol, that penetrates the HA solvation shell in much less extent than dioxane (see also the discussion in section 3.6), it is so intense that almost no difference between the maximum concentrations of water in HA vicinity is observed, no matter what its free-solvent concentration is.

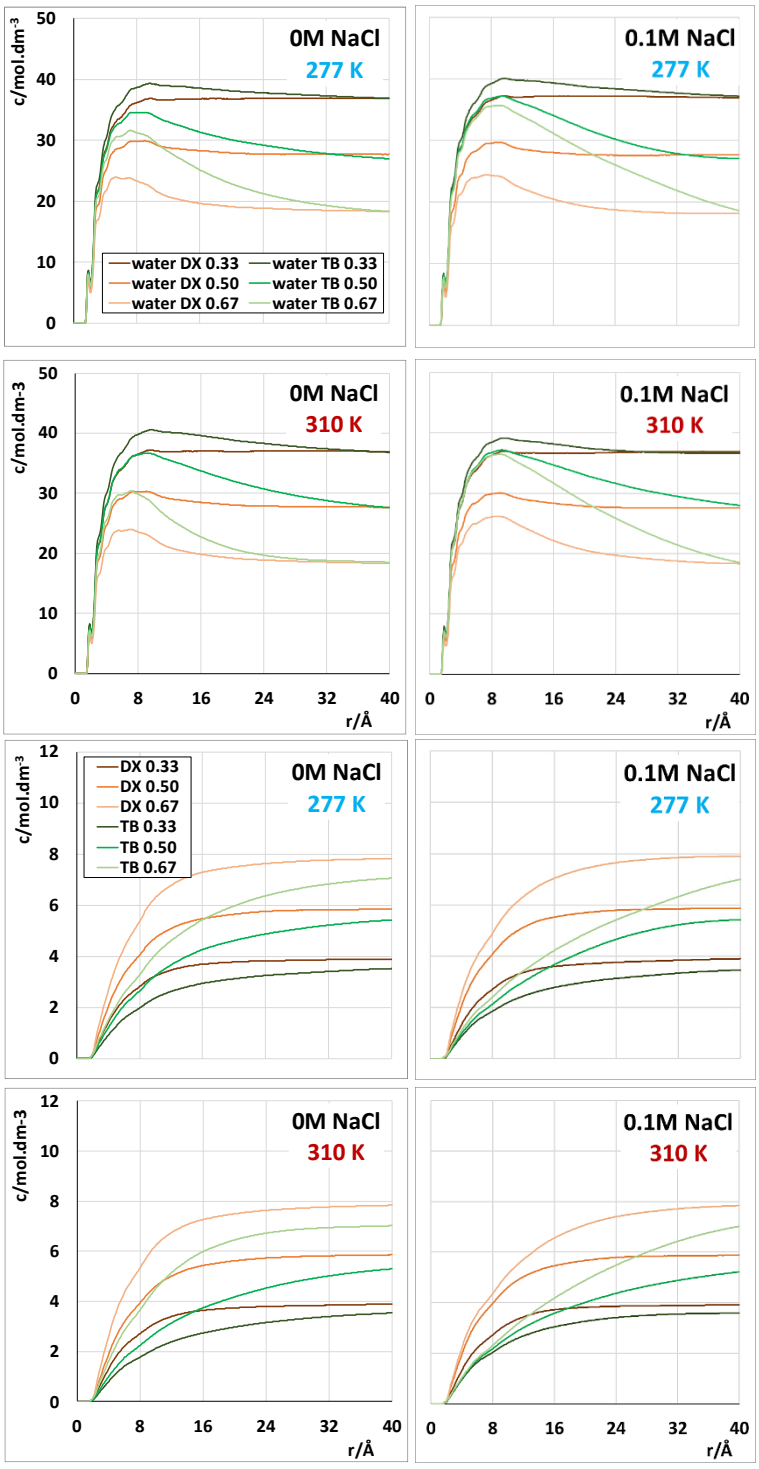

Fig. 2. Molar concentration of water (upper quartet) and the organic component (lower quartet) as a function of the distance from the HA molecule. The organic component and its volume fraction are indicated in the legends.

Hence, the local surroundings of the HA molecule in water:tert-butanol mixtures is almost independent of the free-solvent composition within the studied range (tert-butanol volume

fraction 0.33-0.67) when 0.1 M NaCl is added and varies only moderately even when no NaCl is present.

As a consequence of the different strengths of the solvent separation, the HA solvation shell in tert-butanol solutions is remarkably thicker than in those with dioxane. Considering the organic-component RDF value of 0.95 as the solvation-shell border, in dioxane solutions it is generally below 24 Å, while in their tert-butanol counterparts it is 4-12 Å farther. This indicates remarkably less polar local environment of HA in the dioxane solutions which may positively influence the chemical reactions of HA with non-polar organic substituents, as shown previously (Kutálková et al., 2021; Štrympl et al., 2021).

3.2.Distributions of solvent molecules around the individual residues

Distributions of the different solvent molecules around the individual HA residues, glucuronic acid (GCU) and *N*-acetyl-D-glucosamine (NAG), were studied with the aid of cumulative solvation-shell diagrams (CSSDs). Firstly, the distributions of water were evaluated for all the solvent compositions and both the temperatures (Fig. S1). The diagrams show a strong orientation of hydrogen-bonded water molecules interacting with the hydroxyl groups of HA while in the partially hydrophobic regions in the directions of the axial bonds of the residue rings ("above" and "below") the water molecules are randomly oriented.

The distribution of the organic components follows the distribution of water. In the hydrophilic region of the oxygens O2 and O3 of GCU and O4 and O6 of NAG the organic molecules compete with water for the formation of hydrogen bonds with HA. Similarity of the situation for dioxane and tert-butanol (see Fig. 3 for the organic-component volume fraction of 0.67 and Fig. S2 for the other systems) indicates that the higher probability of dioxane coordination to this position, given by two oxygen atoms in a molecule, is compensated by the

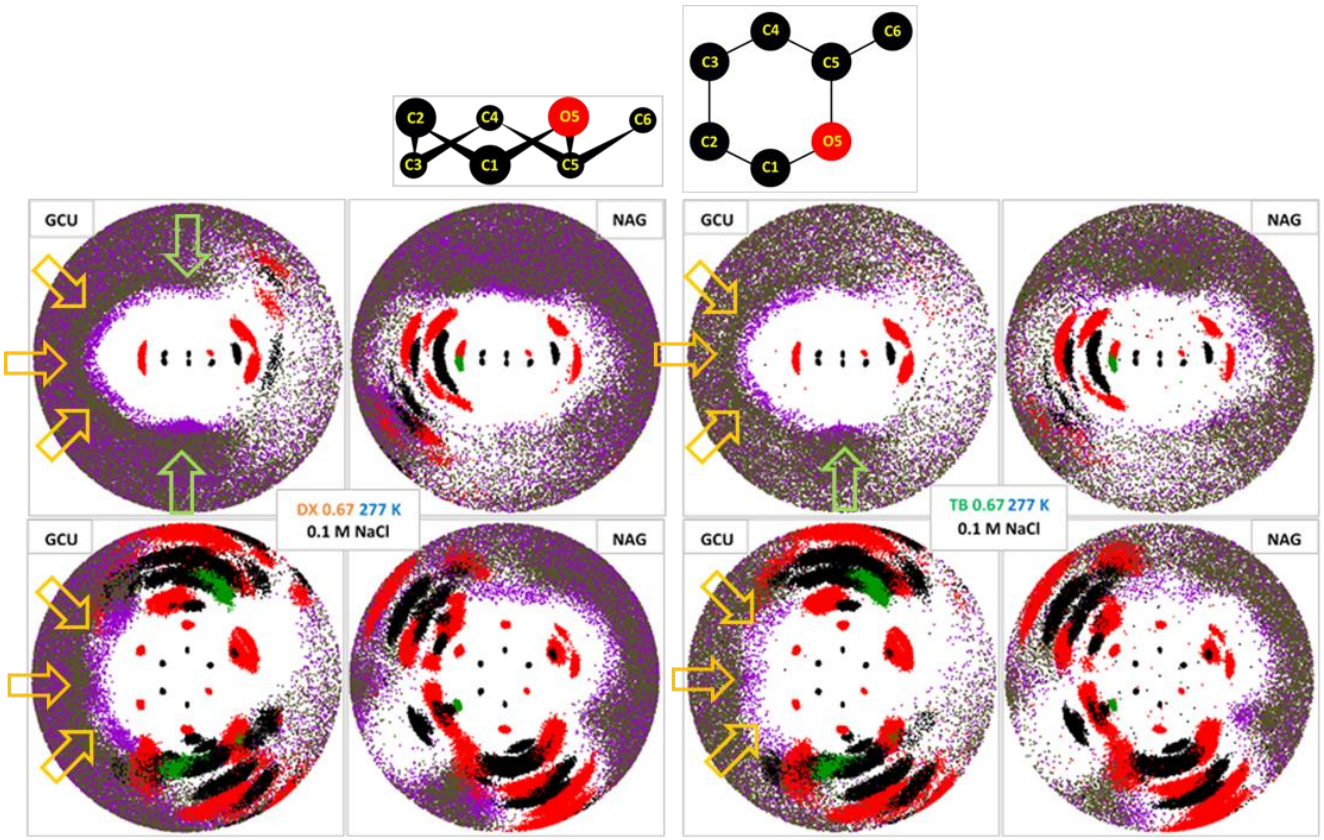

Fig. 3. CSSDs showing the distribution of organic components of the mixed solvents around the HA residues (dioxane – left quartet, tert-butanol – right quartet). The location of individual atoms in the side view (upper images) and top view (lower images) is indicated in the orientation schemes of the monosaccharide ring. Different atoms are shown in specific colors: black – carbon of HA, red – oxygen of HA, green – nitrogen of HA, brown – carbon of organic component, violet – oxygen of organic component. Yellow arrows – region of hydrogen bonded organic molecules, green arrows – organic molecules concentrated at the hydrophobic regions of HA.

hydrogen-bond donor capability of tert-butanol. On the contrary, none of the organic compounds interacts significantly with the carboxylate group. In case of dioxane, it is disabled by the absence of hydrogen-bond donors on both the partners. Tert-butanol may interact, in principle, by its hydroxyl group, but it is expelled from this hydrophilic region by the more strongly interacting water molecules.

In the hydrophobic regions specific locations of the organic-component accumulation occur. The most typical position is below the GCU ring (see Fig. 3) where the organic component concentrates with the oxygen atom oriented towards the GCU residue. This phenomenon is apparent for both the organic compounds, but for dioxane seems to be somewhat stronger. A

similar accumulation is observable also on the other side of the GCU ring, but in a lesser extent. On the NAG residue this effect is considerably weaker and occurs in a higher extent at the opposite ("upper") side of the residue. In accordance with the GCU case, in dioxane solutions it is stronger in comparison with tert-butanol. The concentration of the organic compounds in these hydrophobic regions is likely driven by the hydrophobic interaction pushing the less polar organic molecules towards the non-polar parts of the monosaccharide rings. The fact that the hydrophilic oxygen atom is oriented towards the hydrophobic part of the residues is probably a consequence of steric factors determining the orientation. In case of dioxane this hydrophobic force pushes the four carbons and the related hydrogens to the "parallel" position with respect to the residue ring, while the oxygens tend to stay solvated in the solution. Combination of these effects results in the orientation when one oxygen is in the solvent and the hydrophobic part is closer to the residue, therefore, the other oxygen atom has no other option than being close to the residue ring. Although tert-butanol has only one oxygen atom, its orientation with this atom towards the HA residue is probably enforced by the formation of short-lived hydrophobically stabilized complexes of two tert-butanol molecules supported by their higher concentration in this region. These complexes have two hydroxyl groups on the opposite ends and thus behave similarly as dioxane molecules. Moreover, the expected direct hydrophobic interaction of the three methyl groups with the HA ring is likely in a steric conflict with the hydrophilic regions occupied by the hydrogen-bonded water molecules.

3.3.HA-ions interactions

Previously we showed (Kutálková et al., 2021) that the mixed solvents considerably enhance the interaction between HA and positively charged ions influencing thus the course of chemical reactions containing cationic intermediates. Here we study the interaction of the HA

molecule with mixed solvents in more detail by means of RDFs of Na^+ and Cl^- ions. Time dependences of the number of Na^+ ions within the distance of 4 Å from HA indicate a good equilibration of the ions distribution within the last 100 ns of the simulation for all the systems (Fig. S4). While in aqueous solutions the interactions of Na^+ with HA are rather infrequent unless the NaCl concentration is relatively high (Kutálková et al., 2020), in the mixed solvents their affinity to HA grows substantially. Fig. 4 shows that the frequency of interactions of HA and ions, especially Na^+, is almost independent of temperature except for the pure aqueous solution and, in a lesser extent, the water:dioxane solution of the lowest dioxane concentration.

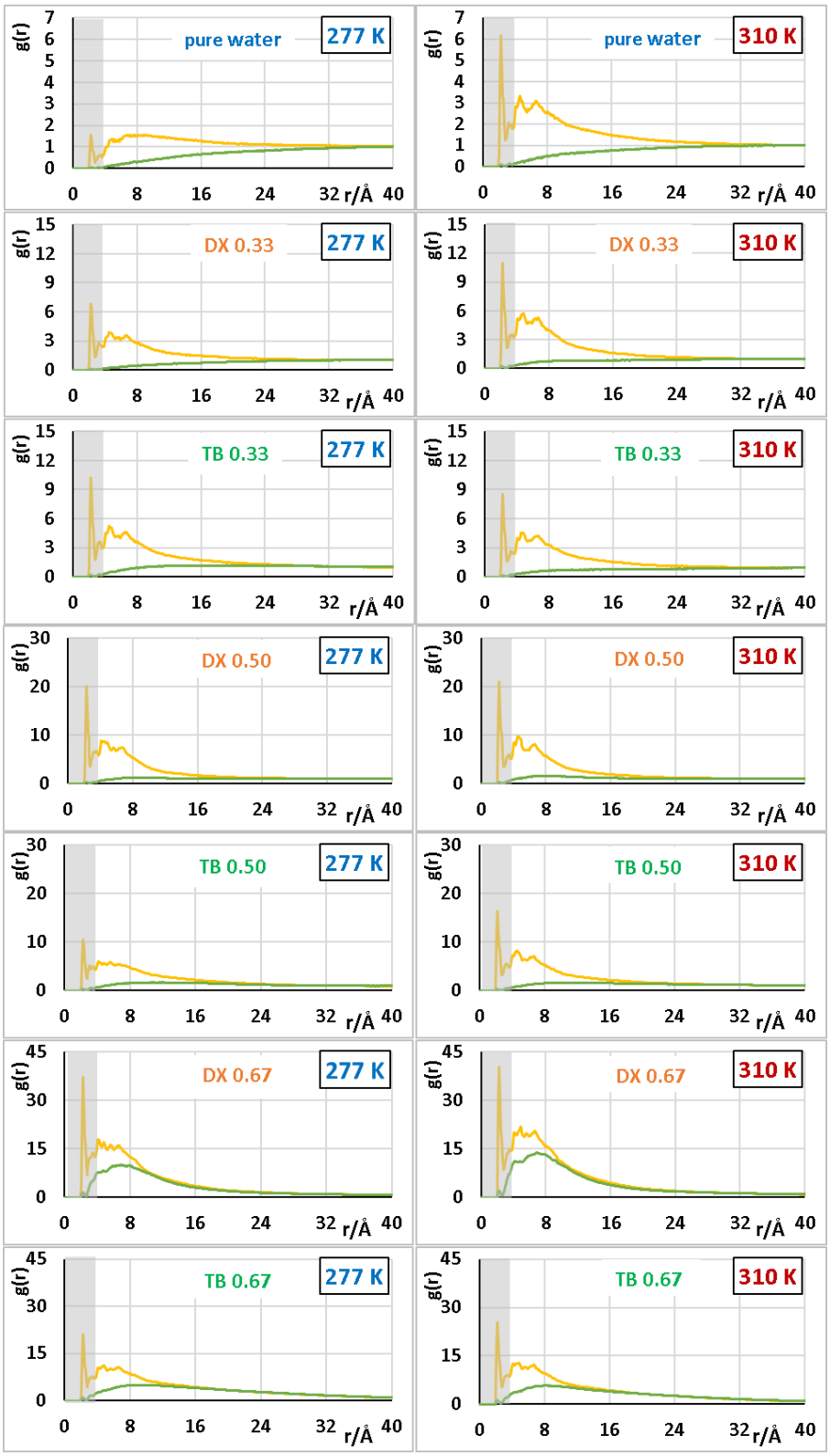

Fig. 4. Radial distribution functions of ions surrounding the HA molecule (Na^+ – yellow, Cl^- – green) at 0.1 M NaCl. The solvent compositions are indicated in the panels (DX – dioxane, TB – tert-butanol). Gray stripe indicates the distance up to 4 Å, compare with Fig. S3.

289

290 In these cases more Na^+ ions interact with HA at the higher temperature indicating the

entropic stabilization of this interaction consisting in the decay of the solvation shell of both the ion and the interacting group on HA, most often the carboxylate group. At higher organic-compounds fraction the permittivity of the solvent decreases lowering the electrostatic screening and thus causing stronger attraction between the Na^+ cations and the negatively charged HA. Therefore, the growing enthalpic component of the Gibbs free energy balances the entropic contribution making thus the Na^+-HA interactions temperature independent. Fig. S3 shows the mean numbers of Na^+ ions within the distance of 4 Å from the HA molecule both with and without 0.1 M NaCl. The stabilizing effect of the organic component is clearly apparent in both the systems. In addition, in the NaCl-containing solutions with the highest organic fraction the numbers of Na^+ cations in this range is even higher than 10, i.e. than the number of carboxylate groups, indicating interactions also at different positions. Indeed, the CSSDs (Fig. 5 and S5) show that Na^+ cations often occupy also the position at the hydroxyl groups on C2 and C3 of GCU (position 2) as well as the positions at the hemiacetal oxygen atoms O5 of the monosaccharide ring of GCU (position 3) and NAG (position 3'). The position at the carboxylate group is denoted as 1. While in aqueous solutions the occupancy of positions 2, 3, and 3' is very low, in both kinds of the mixed solvents they are occupied much more frequently. The difference is especially obvious at the position 3' on the NAG residue occupied only marginally in aqueous solution but reaching almost equal value as the position 3 in the mixed solvents.

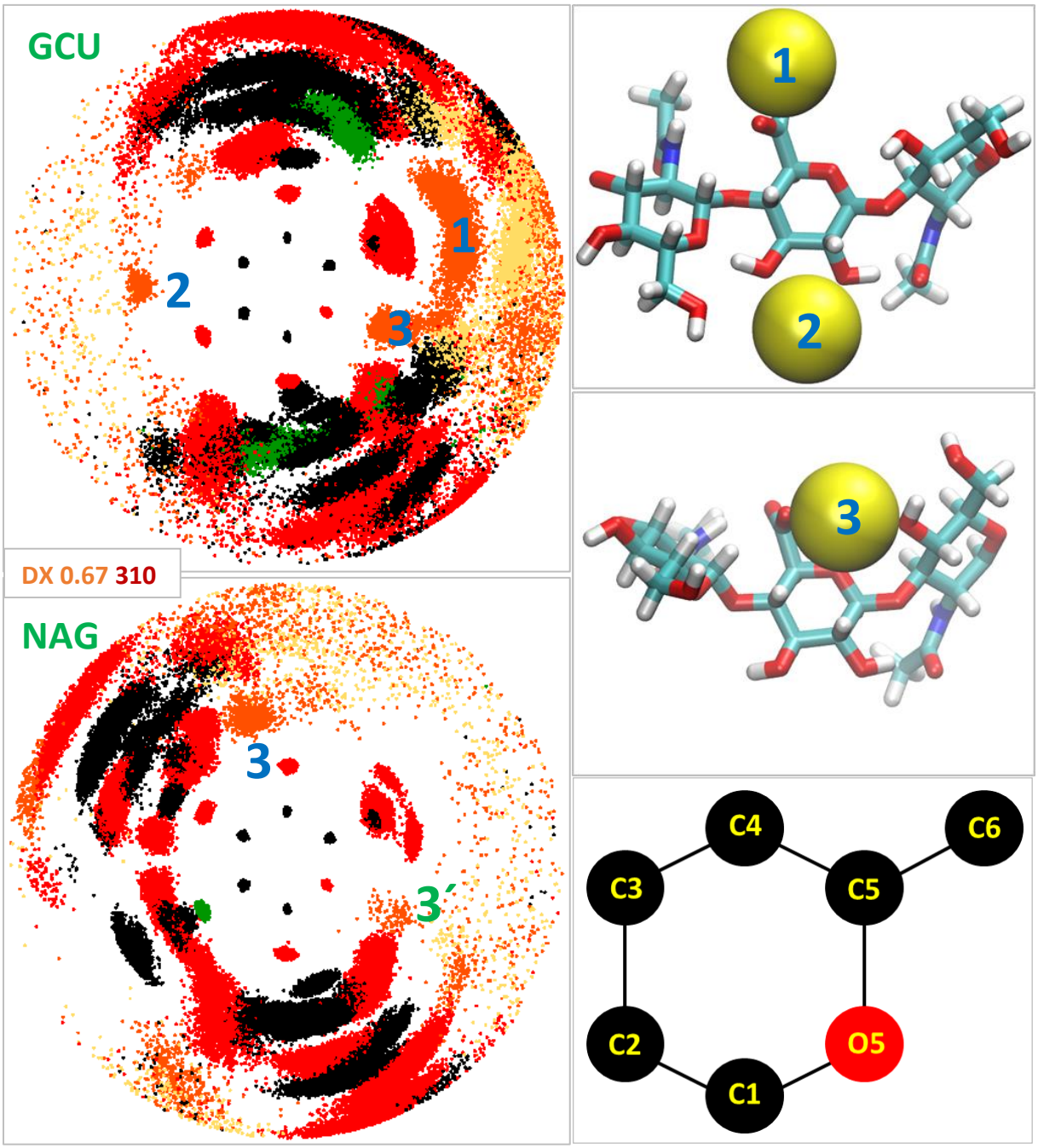

Fig. 5. Cumulative solvation-shell diagram of the ions (Na^+ – orange, Cl – yellow)surrounding the residues of HA molecule for 310 K and the 0.67 dioxane volume fraction. The colors of HA atoms: carbon – black, oxygen – red, nitrogen – green (hydrogen not shown). The positions of frequented locations of Na^+ ions are labeled by numbers (see the main text) and are schematically shown in the two right upper panels. Position 3' is analogous to 3, but located on NAG. Right bottom panel contains the orientation scheme of the residue identifying their location in CSSDs.

311

312 The behavior of the HA molecules in solution is strongly determined by their total charge

313 including the ions present in their solvation shell. Fig. 6 shows this charge, as a function of

314 the distance r from the molecule up to which the ions are included. The total charge grows

along with the distance r from the value of –10 (HA charge) relatively slowly as the attracted Na^+ cations are immediately followed by Cl^- anions, therefore even at 40 Å from HA the total charge is still between –4.0 and –1.5 for all the systems. It indicates that even in the mixed solvents with 0.1 M NaCl HA does not lose its negative charge and keeps its capability to resist precipitation.

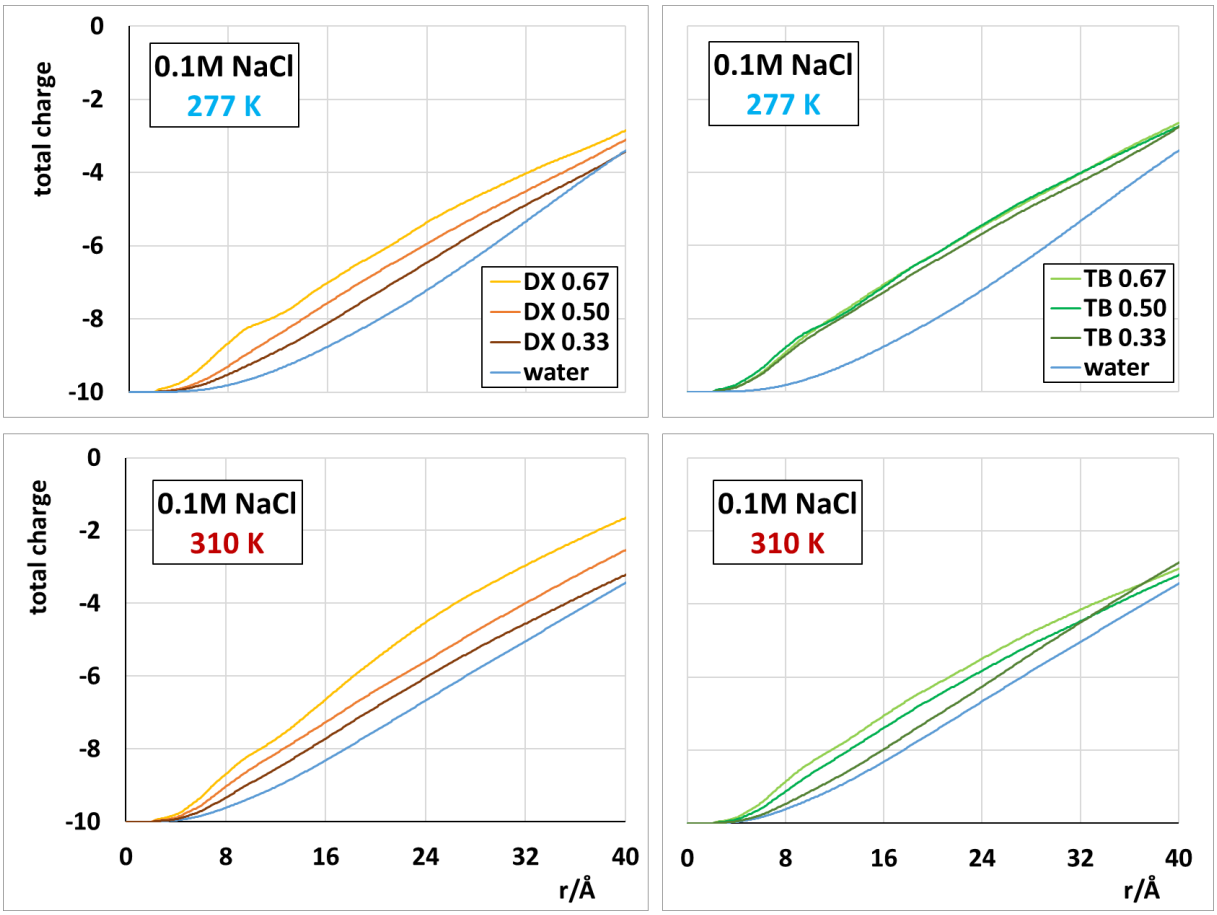

Fig. 6. Total charge of the HA oligosaccharide including its solvation shell up to the distance r. Volume fraction of the organic component (dioxane – left, tert-butanol - right) is indicated in the legends. The pure-water curves are identical for the panels of equal temperature.

An interesting difference between both kinds of solvents can be seen at 277 K. In the solvent series containing pure water and mixtures of 0.33, 0.50 and 0.67 volume fractions of dioxane the negative HA charge at any distance r is compensated in approximately equal steps. In an analogous tert-butanol series the charge of the solvated HA is equal in all the mixed solvents,

sharply distinct from pure water. This is a direct consequence of the strong solvent separation in the tert-butanol solutions resulting in almost composition-independent local environment wrapping HA, as discussed in section 3.1. At the higher temperature the curves of the dioxane-containing solutions are only slightly more separated, while those of tert-butanol lose their uniqueness and depart from each other in the same concentration trend as for their dioxane counterparts, but with lower differences. This is a result of the more rapid thermal motion disrupting the hydrophobic interactions among tert-butanol molecules diminishing thus the solvent-separation strength and allowing more tert-butanol molecules to penetrate the solvation shell of HA, especially when their concentration is high.

3.4.Hydrogen bonds in mixed solvents

Hydrogen bonds constituted by HA can be divided into three groups – intramolecular HA-HA, HA-water, and HA-organic-component. Their average numbers within a simulation time interval are shown in Fig. S6. Obviously, in the salt-free solution the number of HA-water hydrogen bonds decreases along with the growth of the organic-component fraction. The decrease is deeper in the mixtures of dioxane, consistently with its higher occurrence in the solvation shell. The number of these bonds also decreases with the growing temperature almost independently of the solvent composition. The missing HA-water hydrogen bonds are partially compensated by the formation of the HA-organic-component hydrogen bonds. Their number, however, is rather low, therefore only up to one third of the gap is filled this way, often even less. Despite tert-butanol's lower occurrence in the solvation shell, it forms more hydrogen bonds with HA than dioxane as a consequence of its ability to serve both as a donor and acceptor of hydrogen. Finally, the number of the intramolecular hydrogen bonds grows with the organic-component fraction, too. This growth is higher for dioxane, consistently with the decrease of the HA-water hydrogen bonds.

Addition of 0.1 M NaCl does not affect the trends but changes their extent moderately. The number of HA-water hydrogen bonds is generally lower in all the solutions and its decrease along with the growing organic fraction is also steeper. Therefore, the largest differences between salt-free and salt-containing systems can be found in the organic-rich mixtures. This is likely caused by the interference of Na^+ ions with the formation of hydrogen bonds. On the contrary, the influence of NaCl on the intramolecular and HA-organic-component hydrogen bonds is relatively small, partially decreasing their number with respect to the salt-free solution. For the intramolecular hydrogen bonds their initial increase along with the organic-component fraction is even revered to decrease above the value of 0.5.

Increasing temperature lowers the number of HA-water hydrogen bonds in all the systems, as we reported previously for aqueous solutions (Kutálková et al., 2020). The observed decrease differs for different environments but in general stays between 10-20 % of the value for 277 K. A similar decrease can be observed also for the HA-organic-component hydrogen bonds. This indicates the enthalpic stabilization of these bonds resulting in their disturbance by the more intense thermal motion. On the contrary, there is almost no temperature dependence of the number of intramolecular hydrogen bonds within the HA chain. The formation of these bonds is especially supported by the concentration of water molecules in the close surroundings of HA, which is also negligibly temperature dependent. Moreover, the conformation of the HA chain is rather rigid and the thermal motion is unable to change the number of positions prone to hydrogen-bond formation considerably.

3.5.Dynamics of the HA chain in mixed solvents

As we showed previously (Ingr et al., 2017; Kutálková et al., 2020), in pure water the HA chain is relatively rigid forming large and loosely packed random coils. This semirigidity of the chain, indicated by an exponent of the dependence of the radius of gyration on molecular weight higher that 0.5, is typical also for different hydrophilic polysaccharides, see e.g. (Xu et

al., 2012). The rigidity decreases when salt is added to the solution since the cations interacting with the HA chain provoke dynamic processes leading to the formation of temporary hairpin-like kinks and thus partial shrinkage of the random coils. It was also shown that the formation of the kink is often triggered by a flip of a certain glycosidic dihedral angle, most frequently 14_2 (for the labeling of dihedral angles see Fig. S7), following the interaction of the chain with a Na^+ cation, especially when the ion enters the position 3. In the mixed solvents at the lower temperature of 277 K the changes in the chain rigidity, monitored by the mean end-to-end distance of the chain, are relatively small irrespectively of the solvent composition. The differences become more significant when the temperature is increased to 310 K. At this temperature in the presence of 0.1 M NaCl the end-to-end distance apparently decreases along with the growth of the organic-component fraction after a shallow maximum at the organic volume fraction 0.33 (Fig. 7). This decrease is a consequence of more frequent interaction of HA with Na^+ cations leading to the repeated shortenings of the chain, as discussed above. These processes are clearly observable in the correlation of time dependences of certain glycosidic dihedral angles and the end-to-end distance (Fig. S8) confirming our previous findings for aqueous solutions (Kutálková et al., 2020). In addition to that study, in mixed solvents not only 14_2 dihedrals undergo the flips inducing the kink formations but also dihedrals 13_1 contribute to these events. This is probably given by the more frequent occurrence of Na^+ cations in the position 3’ at the hemiacetal oxygen of NAG in mixed solvents. While its GCU counterparts, position 3, provokes the flips in the 1-4 connection, position 3’ does the same in the connection 1-3.

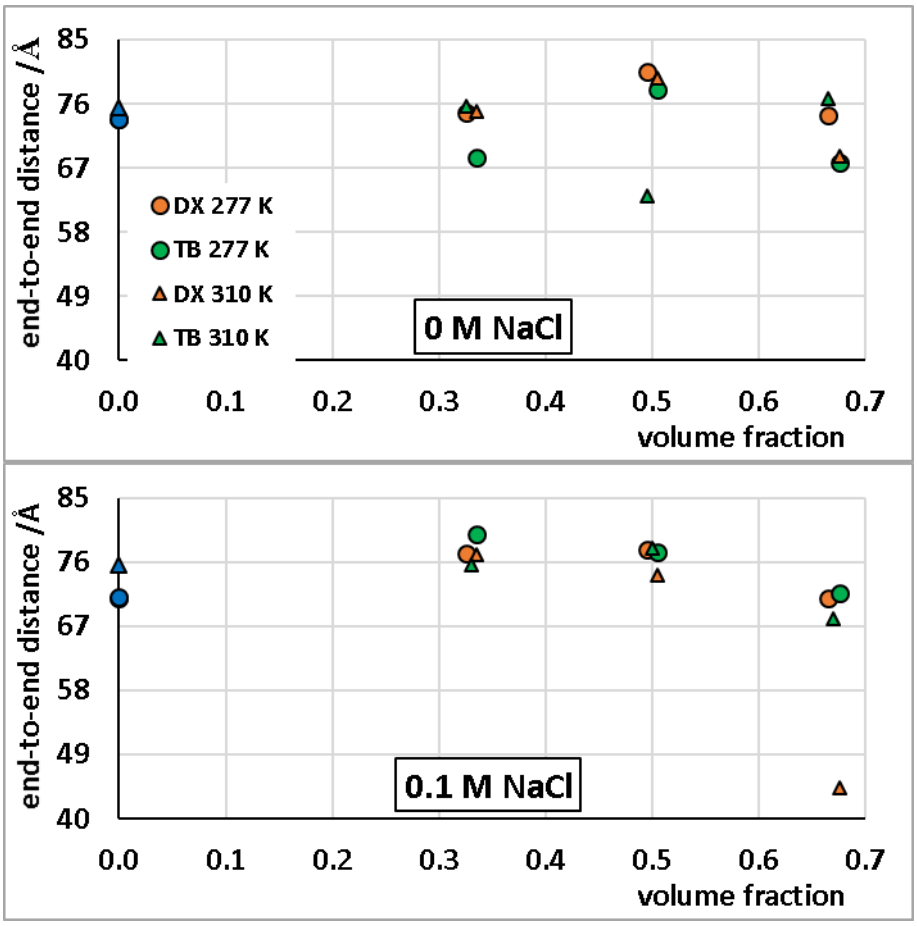

Fig. 7. End-to-end distance of the HA oligosaccharide at different mixed solvents, two NaCl concentrations and two temperatures. Blue points indicate aqueous solution.

As more Na^+ cations occur in the close proximity of HA in dioxane-containing solutions, this phenomenon is stronger there and the end-to-end distance is shorter in comparison with the tert-butanol-containing solutions. The small increase of the end-to-end distance between pure water and organic-component volume fraction of 0.33, where still not much more Na^+ cations approach HA, may be rather attributed to the decrease of permittivity of the solvent leading to a stronger electrostatic repulsion of the charged carboxylate groups in the mixed solvent compared to pure water. This may lead to a more straight and rigid conformation of the HA chain. At the lower temperature of 277 K such a strong dependence is not observed. The probable cause of this is the lower energy of the thermal motion of the molecules. Therefore, even though the number of Na^+ cations interacting with HA, and thus supporting the dihedral

flips, is similar at both the temperatures, the mean kinetic energy of the chain is not sufficient to overcome the energetic barriers of the dihedral rotation very often.

The other studied systems, i.e. at the low temperature or without NaCl, show only much less pronounced dependences on the mixed-solvent composition. Nevertheless, they are also driven by the same phenomena, the frequency of occurrence of the Na^+ cations in the HA solvation shell and the decrease of electrostatic screening. The latter effect is the probable cause of the longer end-to-end distance in all salt-free dioxane solutions compared to those containing tert-butanol. The lower electrostatic screening is given by a weaker solvent separation of dioxane-containing solution, as discussed in section 3.1. The maximum at a certain water:organic volume ratio may correspond with the best combination of the decreasing electrostatic screening and growing interaction of HA with Na^+ cations. The salt-free systems at 310 K show a reversed trend of the tert-butanol-containing solutions compared to those with dioxane that keep a similar profile like at 277 K. Although the explanation of this feature is somewhat questionable, the minimum at the tert-butanol volume fraction of 0.50 may be attributed to the still high electrostatic screening decreasing the rigidity of the chain and already relatively frequent interactions with the Na^+ cations.

3.6.Thermodynamic background of the solvent separation

The phenomenon of the solvent separation can be described by means of chemical potentials of the solvent components. The chemical potential μ_i of a given component is constant throughout the whole system and it can be split to two parts, ideal and non-ideal (excess)

$$\mu_i = \mu_i^{id} + \mu_i^E, \qquad (1)$$

where

$$\mu_i^{id} = \mu_i^0 + RT \ln c_{ri}. \quad (2)$$

Here μ_i^0 is the standard chemical potential of a given component (standard state is pure compound at a given pressure and temperature) and $c_{ri} = c_i/c_i^0$ is the relative concentration of the component defined as the ratio of its concentration in the solution c_i and as a free compound c_i^0. (Defining μ_i as a function of c_{ri} seems to be more convenient in this case compared to the usually used molar fractions due to the local variations of density.) The excess part can be expressed as

$$\mu_i^E = RT \ln \gamma_i(c_{ri}) \quad (3)$$

where $\gamma_i(c_{ri})$ is an activity coefficient of the component dependent on c_{ri}. The non-standard part of the chemical potential

$$\Delta\mu_i = \mu_i - \mu_i^0 = RT \ln c_{ri} + RT \ln \gamma_i(c_{ri}) = const. \quad (4)$$

is constant throughout the whole solution and thus can be calculated from the known free-solvent concentrations of the components far from the HA molecule from the published values of activity coefficients, (Goates & Sullivan, 1958) for dioxane and (Koga et al., 1990) for tert-butanol solutions. In Fig. 8 μ_i^E calculated from the experimental value of $\Delta\mu_i$ and the simulation data

$$\mu_{i,sim}^E = \Delta\mu_i - \mu_i^{id} = \Delta\mu_i - RT \ln c_{ri}(r) \quad (5)$$

is compared with an analogous value calculated from the literature data for the free mixture of the same composition

$$\mu_{i,free}^E = RT \ln \gamma_i\big(c_{ri}(r)\big). \quad (6)$$

Both the quantities defined by equations 5 and 6 are thus considered as functions of the distance from HA molecule r. (As $\mu_{i,sim}^E$ is almost independent of temperature and NaCl

concentration, individual systems will not be distinguished in this discussion; $\Delta\mu_i$ and $\mu^E_{i,free}$ were calculated using the only available data for 298 K and 0 M NaCl.)

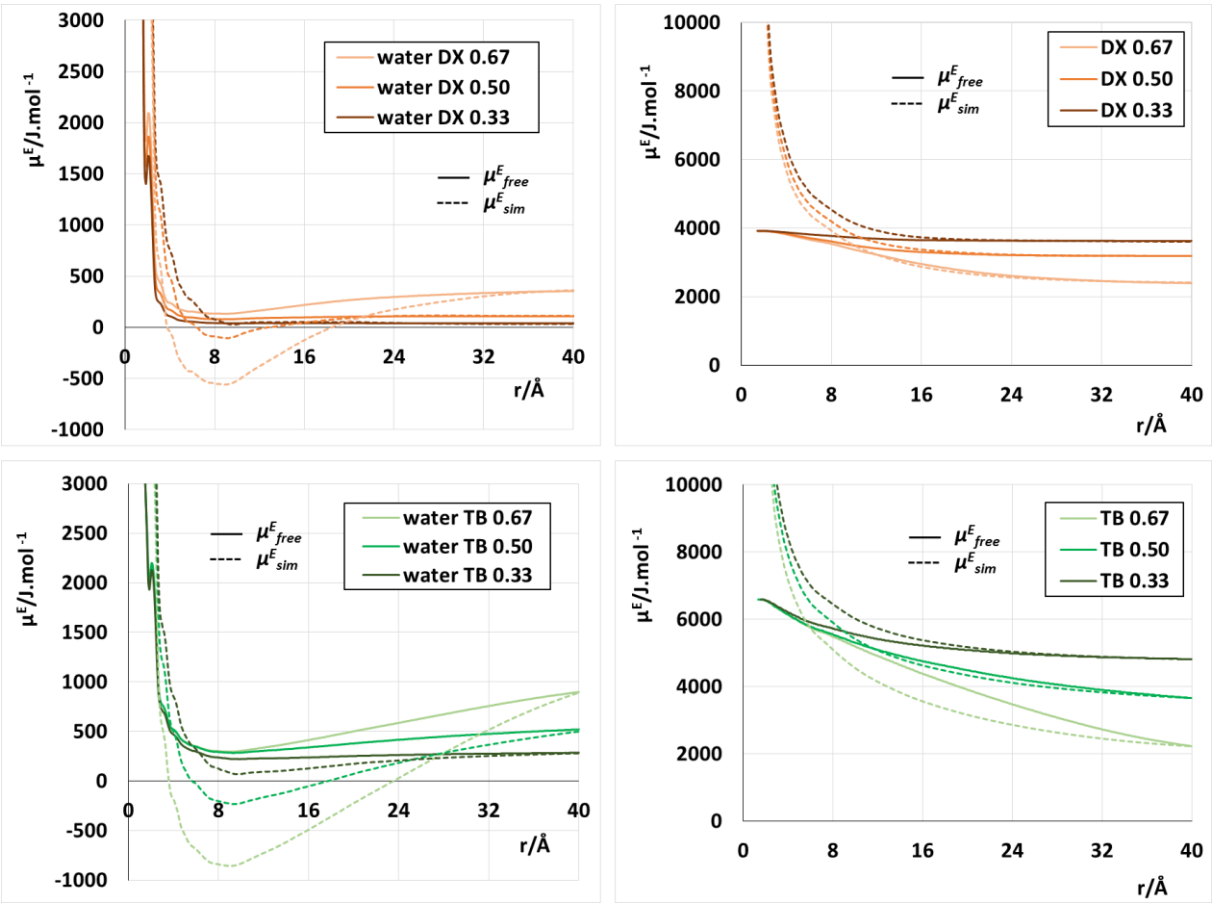

Fig. 8. Excess chemical potentials of water (left) and the organic components (right) determined from the simulation (dashed lines) and calculated for the free solvent from the literature data (solid lines). Dioxane – upper panel, tert-butanol – lower panel. Organic-component volume fractions are indicated in the legends.

This comparison shows that $\mu^E_{i,sim}$ is considerably lower than $\mu^E_{i,free}$ indicating a strong attraction of water by the hydrophilic HA molecule. On the contrary, except the very close vicinity of HA ($r < 10$ Å), where steric hindrances play role, both the potentials are very similar for any of the organic components showing thus very low interaction between HA and the organic compound. The only observable difference for the tert-butanol volume fraction of 0.67 likely originates from an osmotic effect caused by the strong local separation of the components. The organic-component chemical potential is therefore mostly given by the

462 concentrations and behaves like in the free mixture. Consequently, the interaction between
463 HA and water is the primary effect controlling the solvent separation. The differences
464 between dioxane and tert-butanol are rather given by the different absolute values of their
465 excess chemical potentials. For both of them it is positive, but for tert-butanol it is remarkably
466 higher and also grows more steeply with the increasing water content than for dioxane, i.e.
467 with the decreasing distance from the HA molecule. Therefore, due to the primary excess of
468 water molecules at HA tert-butanol has a higher tendency to migrate away from the HA
469 molecule. The molecular reason of this difference consists in the amphiphilic nature of tert-
470 butanol in contrast to the symmetric dioxane molecule, as discussed in section 3.1. The
471 asymmetric tert-butanol molecules are prone to clustering via their hydrophobic parts,
472 therefore they tend to move away from the water-rich region around HA containing a lack of
473 clustering partners. On the contrary, the approach of the hydrophobic parts of dioxane
474 molecules necessarily causes also the approach of the hydrophilic oxygen atoms which have a
475 strong tendency to be solvated by water molecules resulting in their separation and lower
476 tendency to interact with another such molecule. Finally, the similarity of $\mu_{i,sim}^{E}$ and $\mu_{i,free}^{E}$
477 for both the organic components proves the correctness of the force fields used for their
478 molecules.

479

480 ## 4. Conclusions

481 MD simulations of HA oligosaccharides in mixed solvents water:dioxane and water:tert-
482 butanol, in both cases of three different compositions, were carried out. They show a
483 remarkable separation of the mixed-solvent components in the close surroundings of the HA
484 molecule. Primarily, water is attracted by HA and the less polar organic component is repelled
485 from it consequently. A significant difference can be observed between dioxane- and tert-

butanol-containing solutions. Separation of water:dioxane solution is weaker regarding both the concentration changes and their reach from the HA molecule. Tert-butanol-containing solutions, separate more intensively due to the stronger influence of the concentration changes on the tert-butanol chemical potential, likely given by the mutual hydrophobic interactions between the tert-butanol molecules. Dioxane, on the contrary, shows solvent-composition-independent distribution curves indicating the independent behavior of its molecules. Presence of the organic component in the solvent supports the interaction of HA with Na^+ cations, more intensely in the dioxane case due to the weaker solvent separation and thus less polar environment in the close surroundings of HA. In contrast to pure aqueous solutions, the ions bind more frequently to the positions close to the hemiacetal oxygen atoms of both the residues. These HA-Na^+ interaction then induce more frequent flips of the dihedral angles of the glycosidic connections of the residues – not only of the 1-4 connection (flipping almost exclusively in aqueous solutions), but also 1-3. This leads to an apparent shortening of the end-to-end distance of the oligosaccharide observed at the highest organic-component fraction and 0.1 M NaCl and further supports the previously proposed shortening mechanism based on the repeated formation and decay of temporary hairpin-like structures. Although only indirect comparison of our findings with experiment is possible, comparison of the determined excess chemical potential of the organic component with its free-solvent value (Goates & Sullivan, 1958; Hichri et al., 2014; Koga et al., 1990) shows an excellent agreement. Additionally, the agreement of the simulated variations in reactivity of HA with the positively charged intermediates of substitution reactions with experiment (Kutálková et al., 2021; Štrympl et al., 2021) was shown previously.

509 Acknowledgements

510 Computational resources were supplied by the project “e-Infrastruktura CZ” (e-INFRA
511 CZ LM2018140) supported by the Ministry of Education, Youth and Sports of the Czech
512 Republic. This work was supported by the Ministry of Education, Youth and Sports of the
513 Czech Republic through the e-INFRA CZ (ID: 90140). This work was also supported by the
514 internal funding agency of Tomas Bata University in Zlín, no. IGA/FT/2016/011,
515 IGA/FT/2017/009 and IGA/FT/2018/010 to RW, and IGA/FT/2021/010 and
516 IGA/FT/2022/009 to AK.

517

518 References

519 Bakulin, I., Kondratyuk, N., Lankin, A., & Norman, G. (2021). Properties of aqueous 1,4-
520 dioxane solution via molecular dynamics. *The Journal of Chemical Physics*, *155*(15),
521 154501. https://doi.org/10.1063/5.0059337
522 Bełdowski, P., Mazurkiewicz, A., Topoliński, T., & Małek, T. (2019). Hydrogen and Water
523 Bonding between Glycosaminoglycans and Phospholipids in the Synovial Fluid:
524 Molecular Dynamics Study. *Materials*, *12*(13), 2060.
525 https://doi.org/10.3390/ma12132060
526 Bicudo, R. C. S., & Santana, M. H. A. (2012). Effects of organic solvents on hyaluronic acid
527 nanoparticles obtained by precipitation and chemical crosslinking. *Journal of*
528 *Nanoscience and Nanotechnology*, *12*(3), 2849–2857.
529 https://doi.org/10.1166/jnn.2012.5814
530 Blundell, C. D., DeAngelis, P. L., & Almond, A. (2006). Hyaluronan: The absence of amide–
531 carboxylate hydrogen bonds and the chain conformation in aqueous solution are

532 incompatible with stable secondary and tertiary structure models. *Biochemical*
533 *Journal*, *396*(3), 487–498. https://doi.org/10.1042/BJ20060085
534 Buhler, E., & Boué, F. (2004). Chain Persistence Length and Structure in Hyaluronan
535 Solutions: Ionic Strength Dependence for a Model Semirigid Polyelectrolyte.
536 *Macromolecules*, *37*(4), 1600–1610. https://doi.org/10.1021/ma0215520
537 Fouissac, E., Milas, M., Rinaudo, M., & Borsali, R. (1992). Influence of the ionic strength on
538 the dimensions of sodium hyaluronate. *Macromolecules*, *25*(21), 5613–5617.
539 https://doi.org/10.1021/ma00047a009
540 Goates, J. R., & Sullivan, R. J. (1958). Thermodynamic Properties of the System Water-p-
541 Dioxane. *The Journal of Physical Chemistry*, *62*(2), 188–190.
542 https://doi.org/10.1021/j150560a011
543 Gribbon, P., Heng, B. C., & Hardingham, T. E. (2000). The analysis of intermolecular
544 interactions in concentrated hyaluronan solutions suggest no evidence for chain-chain
545 association. *Biochemical Journal*, *350*(Pt 1), 329–335.
546 Hayashi, K., Tsutsumi, K., Nakajima, F., Norisuye, T., & Teramoto, A. (1995). Chain-
547 stiffness and excluded-volume effects in solutions of sodium hyaluronate at high ionic
548 strength. *Macromolecules*, *28*(11), 3824–3830. https://doi.org/10.1021/ma00115a012
549 Hichri, M., Besbes, R., Trabelsi, Z., Ouerfelli, N., & Khattech, I. (2014). Isobaric vapour–
550 liquid phase diagram and excess properties for the binary system 1,4-dioxane + water
551 at 298.15 K, 318.15 K and 338.15 K. *Physics and Chemistry of Liquids*, *52*(3), 373–
552 387. https://doi.org/10.1080/00319104.2013.833618
553 Hu, Z., Xia, X., & Tang, L. (2009, October 13). *Process for Synthesizing Oil and Surfactant-*
554 *free Hyaluronic Acid Nanoparticles and Microparticles* [Patent]. UNT Digital Library.
555 https://doi.org/govno: 10/980125

556 Huerta-Angeles, G., Bobek, M., Příkopová, E., Šmejkalová, D., & Velebný, V. (2014). Novel
557 synthetic method for the preparation of amphiphilic hyaluronan by means of aliphatic
558 aromatic anhydrides. *Carbohydrate Polymers*, *111*, 883–891.
559 https://doi.org/10.1016/j.carbpol.2014.05.035
560 Humphrey, W., Dalke, A., & Schulten, K. (1996). VMD: Visual molecular dynamics. *Journal*
561 *of Molecular Graphics*, *14*(1), 33–38, 27–28. https://doi.org/10.1016/0263-
562 7855(96)00018-5
563 Ingr, M., Kutálková, E., & Hrnčiřík, J. (2017). Hyaluronan random coils in electrolyte
564 solutions-a molecular dynamics study. *Carbohydrate Polymers*, *170*, 289–295.
565 https://doi.org/10.1016/j.carbpol.2017.04.054
566 Koga, Yoshikata., Siu, W. W. Y., & Wong, T. Y. H. (1990). Excess partial molar free
567 energies and entropies in aqueous tert-butyl alcohol solutions at 25.degree.C. *The*
568 *Journal of Physical Chemistry*, *94*(19), 7700–7706.
569 https://doi.org/10.1021/j100382a070
570 Kolaříková, A., Kutálková, E., Buš, V., Witasek, R., Hrnčiřík, J., & Ingr, M. (2022). Salt-
571 dependent intermolecular interactions of hyaluronan molecules mediate the formation
572 of temporary duplex structures. *Carbohydrate Polymers*, *286*, 119288.
573 https://doi.org/10.1016/j.carbpol.2022.119288
574 Kutálková, E., Hrnčiřík, J., Witasek, R., & Ingr, M. (2020). Effect of solvent and ions on the
575 structure and dynamics of a hyaluronan molecule. *Carbohydrate Polymers*, *234*,
576 115919. https://doi.org/10.1016/j.carbpol.2020.115919
577 Kutálková, E., Hrnčiřík, J., Witasek, R., Ingr, M., Huerta-Ángeles, G., Hermannová, M., &
578 Velebný, V. (2021). The rate and evenness of the substitutions on hyaluronan grafted
579 by dodecanoic acid influenced by the mixed-solvent composition. *International*

Journal of Biological Macromolecules, *189*, 826–836. https://doi.org/10.1016/j.ijbiomac.2021.08.137

Mendichi, R., Soltés, L., & Giacometti Schieroni, A. (2003). Evaluation of radius of gyration and intrinsic viscosity molar mass dependence and stiffness of hyaluronan. *Biomacromolecules*, *4*(6), 1805–1810. https://doi.org/10.1021/bm0342178

Overduin, S. D., Perera, A., & Patey, G. N. (2019). Structural behavior of aqueous t-butanol solutions from large-scale molecular dynamics simulations. *The Journal of Chemical Physics*, *150*(18), 184504. https://doi.org/10.1063/1.5097011

Payne, W. M., Svechkarev, D., Kyrychenko, A., & Mohs, A. M. (2018). The role of hydrophobic modification on hyaluronic acid dynamics and self-assembly. *Carbohydrate Polymers*, *182*, 132–141. https://doi.org/10.1016/j.carbpol.2017.10.054

Peydecastaing, J., Vaca-Garcia, C., & Borredon, E. (2011). Bi-acylation of cellulose: Determining the relative reactivities of the acetyl and fatty-acyl moieties. *Cellulose*, *18*(4), 1015–1021. https://doi.org/10.1007/s10570-011-9528-9

Phillips, J. C., Braun, R., Wang, W., Gumbart, J., Tajkhorshid, E., Villa, E., Chipot, C., Skeel, R. D., Kalé, L., & Schulten, K. (2005). Scalable Molecular Dynamics with NAMD. *Journal of Computational Chemistry*, *26*(16), 1781–1802. https://doi.org/10.1002/jcc.20289

Schanté, C. E., Zuber, G., Herlin, C., & Vandamme, T. F. (2011). Chemical modifications of hyaluronic acid for the synthesis of derivatives for a broad range of biomedical applications. *Carbohydrate Polymers*, *85*(3), 469–489. https://doi.org/10.1016/j.carbpol.2011.03.019

Scott, J. E., & Heatley, F. (1999). Hyaluronan forms specific stable tertiary structures in aqueous solution: A 13C NMR study. *Proceedings of the National Academy of Sciences*, *96*(9), 4850–4855. https://doi.org/10.1073/pnas.96.9.4850

Scott, J. E., & Heatley, F. (2002). Biological Properties of Hyaluronan in Aqueous Solution Are Controlled and Sequestered by Reversible Tertiary Structures, Defined by NMR Spectroscopy. *Biomacromolecules*, *3*(3), 547–553. https://doi.org/10.1021/bm010170j

Siódmiak, J., & Bełdowski, P. (2019). Hyaluronic Acid Dynamics and its Interaction with Synovial Fluid Components as a Source of the Color Noise. *Fluctuation and Noise Letters*, *18*(02), 1940013. https://doi.org/10.1142/S0219477519400133

Siódmiak, J., Bełdowski, P., Augé, W. K., Ledziński, D., Śmigiel, S., & Gadomski, A. (2017). Molecular Dynamic Analysis of Hyaluronic Acid and Phospholipid Interaction in Tribological Surgical Adjuvant Design for Osteoarthritis. *Molecules (Basel, Switzerland)*, *22*(9). https://doi.org/10.3390/molecules22091436

Štrympl, O., Vohlídal, J., Hermannová, M., Maldonado-Domínguez, M., Brandejsová, M., Kopecká, K., Velebný, V., & Huerta-Ángeles, G. (2021). Oleate-modified hyaluronan: Controlling the number and distribution of side chains by varying the reaction conditions. *Carbohydrate Polymers*, *267*, 118197. https://doi.org/10.1016/j.carbpol.2021.118197

Svechkarev, D., Kyrychenko, A., Payne, W. M., & Mohs, A. M. (2018). Probing the self-assembly dynamics and internal structure of amphiphilic hyaluronic acid conjugates by fluorescence spectroscopy and molecular dynamics simulations. *Soft Matter*, *14*(23), 4762–4771. https://doi.org/10.1039/c8sm00908b

Vítková, L., Musilová, L., Achbergerová, E., Minařík, A., Smolka, P., Wrzecionko, E., & Mráček, A. (2019). Electrospinning of Hyaluronan Using Polymer Coelectrospinning and Intermediate Solvent. *Polymers*, *11*(9). https://doi.org/10.3390/polym11091517

Xu, S., Xu, X., & Zhang, L. (2012). Branching structure and chain conformation of water-soluble glucan extracted from Auricularia auricula-judae. *Journal of Agricultural and Food Chemistry*, *60*(13), 3498–3506. https://doi.org/10.1021/jf300423z

630